Journal of Molecular Catalysis A: Chemical 342–343 (2011) 91–100

Contents lists available at ScienceDirect

Journal of Molecular Catalysis A: Chemical

journal homepage: www.elsevier.com/locate/molcata

Catalytic activity of bifunctional transition metal oxide containing phosphated alumina catalysts in the dehydration of glycerol

Wladimir Suprun*, Michal Lutecki, Roger Gläser, Helmut Papp

Institute of Chemical Technology, Universität Leipzig, D-04103 Leipzig, Germany

ARTICLE INFO

Article history:
Received 7 February 2011
Received in revised form 28 April 2011
Accepted 29 April 2011
Available online 8 May 2011

Keywords:
Transition metal oxide
Al_2O_3-PO_4
Glycerol
Dehydration

ABSTRACT

A systematic study was conducted to evaluate the effect of different transition metal oxide loaded on phosphated alumina as catalysts for the gas-phase dehydration of glycerol. The series of MeO–Al_2O_3-PO_4 catalysts at the constant Me:Al ratio was prepared by impregnation of alumina and characterized with respect to their textural properties, crystallinity, acidity and reducibility. Catalytic performance was tested at the constant operating conditions in the presence of steam. It was found that conversion, and acrolein formation increased with the increase of the total catalyst acidity; i.e., the selectivity to acrolein increased in the order: Ce < Mn < Cr < V ~ Fe < Cu < Mo < W. The highest selectivity towards acrolein (54%) was observed over W contained catalyst after a long-term test, i.e., 30 h. For Ce, Fe and Cr catalysts low selectivity to acrolein (12–23%) was observed. Contrary CuO_x–Al_2O_3-PO_4 catalyst favored the formation of acetol (50%). In the case of Cr-, Mn- and V-containing alumina phosphates an enhanced formation of acetaldehyde and CO_x, was observed as a result of destructive glycerol cleavage. The V- and Fe-containing catalysts promote the formation of allyl alcohol. Finally, the change of the total acidity, oxidation state and crystallinity for spent catalysts was studied by NH_3-TPD, TPO, TPR and XPS analysis. In general, MO–Al_2O_3-PO_4 catalysts showed improved stability against deactivation which can be attributed to the oxidative properties of the transition metal oxide components that enhance coke removal.

1. Introduction

As a renewable feedstock and energy carrier, bio-diesel has attracted much attention [1]. Bio-diesel production results in the accumulation of crude glycerol as a main by-product. With this, it is expected an increasing of the world production of biodiesel, a glut of crude "bio-glycerol" considerably reduced the market prices of raw glycerol (GL). Therefore efficient transformations of cheap bio-glycerol into valuable chemicals are an important goal of current research. Many research groups have focused on utilizing raw glycerol by converting it into fuel additives and fine C_3-chemicals [1]. Another possible use of GL involves its catalytic conversion to acrylic acid, acrolein and hydroxyacetone (acetol) as an alternative to petrochemical routes [2,3]. Acrolein as an important intermediate in the production of acrylic acid, 1,3-propanediol and methionine, is currently produced by gas-phase oxidation of propene with a Bi–Mo–V mixed oxide catalyst [4]. As a sustainable alternative, acrolein can be synthesized by the double dehydration of GL. Therefore the catalytic dehydration of glycerol to acrolein and acetol has gained considerable scientific and industrial interest during the last decade [2,3].

Different solid acid catalysts including zeolites [5–8] and Al_2O_3, TiO_2, ZrO_2 and SiO_2 impregnated with phosphates or sulphates have been proposed for GL dehydration in the gas phase [9–12] or in supercritical water [13]. These catalysts need to overcome various problems such as harsh reactions conditions, rapid catalyst deactivation due to coke deposition and formation of large amounts of undesired by-products. Additionally, various heteropoly acids (HPA) loaded on different supports were intensively investigated for gas phase dehydration of GL [14–17]. However, supported HPA exhibit a limited thermal stability (up to ca. 450 °C) accompanied with progressive deactivation after 5–10 h TOS. Recently, Armbruster et al. [18] showed that dilution of $H_4SiW_{12}O_{40}$–Al_2O_3 catalyst with inert quartz (1:20) results in a long term activity above 250–300 h. However, a strong dilution of HPA catalysts decreases the space-time-yields. In addition, the limited thermal stability (decomposition at >400 °C) of HPA can be also a potential obstacle for its practical application since regeneration of the coked catalyst usually requires temperature higher than 450 °C. To overcome the catalyst deactivation, Dubois et al. [19] and Ulgen and Hoelderich [20] proposed WO_3 as active species on different supports as long term active catalytic systems for gas phase dehydration of GL to acrolein.

In the last decade various bifunctional catalytic systems containing acidic components and transition metal ions were investigated as catalysts for gas-phase dehydration of alcohols [2,3,21–24].

* Corresponding author. Tel.: +49 341 9736300; fax: +49 341 9736349.
E-mail address: suprun@chemie.uni-leipzig.de (W. Suprun).

1381-1169/$ – see front matter © 2011 Elsevier B.V. All rights reserved.
doi:10.1016/j.molcata.2011.04.020

Especially, alumina phosphates have been studied extensively due to their high specific surface area, thermal stability and acid–base properties. In order to further increase or change its acid–base properties, the addition of Na-, K-, Ni- or Fe-, Co-, Mn-, Cu- and Cr-oxides have been proposed [21–25].

Additionally, catalytic conversions of C2–C4-diols were reported using Ce-oxides [26] as well as some of the rare earth pyrophosphates [27].

Generally it is shown in the literature that different catalysts including transition metal oxides such as CeO_2, CuO, WO_3, Fe_2O_3 and CrO_3 are able to catalyze the GL dehydration leading to the formation of acrolein, acetol and/or other by-products. The latter by-products i.e., products of oligomerization and polymerization, are mainly responsible for the deactivation of the catalysts. The problem of deactivation was not extensively discussed in the literature, although several authors proposed an approach which needs to be considered in the future design of the catalysts to avoid extensive coke formation [7,9,12,27,28]. For example, the presence of transition metal ions [19,20,25,29] on supports with adequate acidic properties seems to be a promising concept to catalyze specific reaction pathways involved in the reaction mechanism exclusively leading to acrolein and/or acetol.

Numerous studies suggested that the nature of the acid sites (Brønsted and/or Lewis) would play a key role in determining catalytic performance of solid acids in dehydration of GL [3,7,30–32]. Very recently, Erfle et al. [33] investigated the catalytic activity of Mo, V and Si containing HPA supported on SiO_2–Al_2O_3 in glycerol dehydration using EPR-spectroscopy. It was concluded, that the observed high performance of HPVMo as active phase is due to the high number of surface protons (concentration of Brønsted sites) and that their excess leads to coke formation. Furthermore, it was suggested that the structure of transition metal ions in glycerol dehydration might be less important for catalytic performance in comparison to other proprieties such as pore structure and surface acidity.

Despite the numerous data reported over the last decade on the catalytic dehydration of GL, there still remain important and open questions with respect to the performance of metal oxide-containing bifunctional catalysts:

(i) Why do W- and Mo-oxides (or phosphates) [19,20] predominantly promote a high selectivity to acrolein while Cu- and Ce-oxide favor the dehydration of glycerol to acetol [22,29]?
(ii) Is this effect caused by the "optimal" acidity, optimal size of pore channels, a redox activity (reducibility) or specific coordination properties of these transition metal ions?
(iii) Why do V- and Fe-phosphates, with relatively low surface areas (5–9 $m^2\,g^{-1}$) exhibit high conversion degrees already at 280 °C [30,31]?
(iv) Why do Fe-containing catalysts in form of Fe_2O_3 supported on $Al(H_2PO_4)_3$ [34] or iron phosphate [31] favor different reaction pathways in GL dehydration (i.e., formation of allyl alcohol or acrolein, respectively)? Is this effect caused by the catalyst support, active Fe–species or different reaction conditions?

In an earlier work [28,35,36] we reported about the catalytic properties of various solid acids in the gas-phase dehydration of GL. It was found that mesoporous Al_2O_3-PO_4 was a more effective catalyst with long term stability in comparison to the microporous SAPO-11 and -34 materials. In this work we investigated different transition metal oxides (Cr, Cu, Ce, Fe, Mn, Mo, V and W) loaded on phosphated alumina. The catalysts were prepared by wet impregnation of phosphated γ-Al_2O_3 with the appropriate metal salts and characterized by BET, XRD, XPS, TPD, TPR, and TPO. In order to compare the activity of the catalysts the loading of the transition metals and of the PO_4 component was kept constant. The aim of the present work was to get more insight into the role of surface acid properties and the influence of transition metals on the reaction mechanism. To the best of our knowledge, there is no report in the literature about the catalytic activity of different transition metal oxides loaded on phosphated alumina for catalytic conversion of GL.

2. Experimental

2.1. Catalyst preparation

Phosphated alumina (Al_2O_3-PO_4) was prepared by impregnation of γ-Al_2O_3 (Acros, specific surface area 256 $m^2\,g^{-1}$; mean pore diameter between 115 and 125 Å) with 25 wt% aqueous solution of H_3PO_4 (Acros, 85 wt%). The Al_2O_3-PO_4 were dried at 110 °C for 12 h and calcined in air for 4 h at 520 °C. The preparation of MO_x–Al_2O_3-PO_4 samples was carry out by impregnation of 10 g alumina with 50 ml aqueous solution of the corresponding metal salts and phosphoric acid under constant stirring at 25 °C for 120 min. The atomic relation between metal, alumina and phosphate was kept constant, i.e., Me:Al = 1:10 and PO_4/Al = 1:12. The following metal salts were used for impregnation: $Cu(NO_3)_2{\cdot}3H_2O$, $Ce(NO_3)_3{\cdot}6H_2O$; $Cr(NO_3)_3{\cdot}9H_2O$, $Fe(NO_3)_2{\cdot}9H_2O$, $Mn(NO_3)_2{\cdot}4H_2O$ all from Fluka), ammonium methavanadate (Aldrich) and ammonium molybdate (Aldrich). The impregnated MO_x–Al_2O_3-PO_4 were dried at 110 °C for 12 h and calcined in air for 4 h at 520 °C. Finally all catalysts were pressed, sieved and a fraction with a grain size between 150 and 300 mm was used in the catalytic experiments. The catalyst composition and notation of the prepared samples are listed in Table 1.

2.2. Characterization

Textural properties were determined from adsorption–desorption isotherms of nitrogen at −196 °C using an ASAP 2010 apparatus (Micromeritics). The specific surface areas were determined by applying the BET equation at a relative pressure range of $0.03 \le p/p \le 0.22$.

Powder X-ray diffraction (XRD) patterns were recorded on a Bruker D8 Advance X-ray diffractometer using a nickel-filtered Cu K_α (0.15418 nm) radiation source at 40 kV and 50 mA, respectively.

X-ray photoelectron spectroscopy (XPS) was performed using an X-ray source (Specs GmbH) with Mg anode (1253.6 eV). The spectra analyses including satellites and background subtraction (Shirley) were performed with the CasaXPS software. The binding energy of C 1s BE = 284.6 eV was used as calibration standard for corrections.

Ammonia TPD was performed using a flow microreactor; the evolved gases were analysed with a quadrupole mass spectrometer (Pfeiffer GSD 301). Prior to the analysis, the sample was pretreated in He (50 ml min^{-1}) at 250 °C for 1 h. After cooling down to 95 °C, the adsorption experiments were carried out by consecutive pulses of 1 ml ammonia until a complete saturation of the surface was reached. After the removal of physisorbed ammonia by purging with helium, the sample was heated from 95 up to 600 °C (heating rate: 10 K min^{-1}) in He; desorbed NH_3 was recorded by MS detector (me: 16). The amount of desorbed ammonia was quantified using a reference test, pulsing 1 ml ammonia over 50 mg of inert quartz.

H_2-TPR profiles were obtained with an AMI 100 (Altamira) instrument equipped with a TC detector. The catalysts were pretreated in a nitrogen flow at 300 °C for 30 min and after that cooled down to room temperature. The TPR measurements were recorded from 30 to 800 °C in a H_2/Ar flow (5 vol.% H_2; flow rate: 50 ml min^{-1}, heating rate: 10 K min^{-1}).

Qualitative and quantitative TPO-MS investigations of coke deposits on the used catalysts were performed by thermogravime-

Table 1
Textural properties of fresh and used transition metal-containing phosphated alumina catalysts MO_x–Al_2O_3-PO_4.

Sample	Catalyst notation	PD (Å)[a]	A_{BET} (m^2/g)		ΔA_{BET}	Catalyst acidity (measured by NH_3-TPD)		Coke deposits[f]
			Fresh	Used	(%)[b]	TA[c]	IA[d]	mg C/m^2
γ-Al_2O_3	AO	124	256	78	69	140	0.62	0.03
γ-Al_2O_3-PO_4	APO	115	207	120	42	295/125[e]	1.42	0.45[g]
CuO_x–Al_2O_3-PO_4	Cu-APO	89	190	163	14	382/250[e]	2.49	0.30
CrO_x–Al_2O_3-PO_4	Ce-APO	88	185	148	9	194	1.06	0.13
CeO_x–Al_2O_3-PO_4	Cr-APO	72	211	116	45	193	0.92	0.51
FeO_x–Al_2O_3-PO_4	Fe-APO	90	215	187	13	252	1.21	0.15
MnO_x–Al_2O_3-PO_4	Mn-APO	65	166	151	8	155	0.93	0.18
MoO_x–Al_2O_3-PO_4	Mo-APO	68	163	151	15	369	2.31	0.21
VO_x–Al_2O_3-PO_4	V-APO	80	224	138	9	259/356[e]	1.16	0.22
WO_x–Al_2O_3-PO_4	W-APO	70	158	142	10	468/650[e]	3.15	0.23

[a] Average pore diameter calculated according to the Barret–Joyner–Halenda (BJH) method.
[b] Change of BET area after dehydration reaction at 280 °C for 30 h.
[c] TA: total acidity (micro mol/g).
[d] IA: intrinsic acidity (micro mol/m^2).
[e] Data after back slash were analysed for spent catalyst after 10 h or 30 h of reaction, respectively.
[f] Specific coke amount after 30 h of reaction.
[g] Data analysed after 10 h of reaction.

try using STA-409 (Netzsch) coupled with MS-Analyser (GSD 301; Pfeiffer). The TPO experiments were carried out in the temperature range of 25 to 800 °C with a heating rate of 10 K min^{-1} under air flow of 75 ml min^{-1}. The amount of carbon dioxide formed during combustion of coke was quantified referencing it to thermal decomposition of $CaCO_3$.

2.3. Catalytic experiments

The dehydration of GL was carried out in a continuous flow fixed-bed reactor at atmospheric pressure. A mixture of 200 mg catalyst with inert quartz was packed in a glass reactor (5 mm i.d.) and placed in a vertical furnace. In previous experiments it was shown that the reaction over "dry" catalysts leads to a rapid deactivation and an extensive formation of products of the oxidative cleavage (i.e., CO and CO_2) due to a very strong initial adsorption of glycerol. To minimize this effect, the surface of the catalyst was pre-treated in a stream of He with 15 vol.% water at 280 °C for 15 h. After the hydrothermal treatment, the dehydration reaction was carried out at 280 °C ("standard" reaction temperature in this study). 500 mg h^{-1} of aqueous solution of glycerol (5 wt%) was charged with a liquid flow controller and then evaporated at 200 °C (Bronkhorst) prior to entering the reactor in a down-flow mode. The concentrations of GL and water in the feed were 0.18 vol.% and 15 vol.%, respectively.

In order to quantify the obtained reaction products, the reaction mixture was condensed in a cold trap (−10 °C; aqueous solution of cooled in cryostat Julabo 4B) and collected hourly for off-line GC-analysis. The product samples were analysed without preliminary separation using a gas chromatograph (Chrompack 9001) equipped with a capillary column (OPTIMA-WAX, 30 m MN) and an FID detector, temperature program: 100 °C (2 min), 12 K min^{-1}, 245 °C (5 min). Additionally CO and CO_2 were analysed on-line using the FTIR Gas-Analyser 1301 (INNOVA).Quantification was achieved by mixing 500 μl of condensed reaction mixture and 500 μl of 1 wt% aqueous solution of ethylene glycol as an internal standard. Conversion of GL (X) and product selectivity (S_i) were calculated according to the following Eqs. (1) and (2) [28]:

$$X\ (\%) = \frac{n_{GL}^{input} - n_{GL}^{output}}{n_{GL}^{input}} \times 100 \quad (1)$$

$$S\ (\%) = \frac{n_i}{n_{GL}^{input} - n_{GL}^{output}} \times \frac{Z_i}{Z_{GL}} \times 100 \quad (2)$$

where n_{GL}^{input} and n_{GL}^{output} are the molar streams of GL in the input and output; n_i the molar stream of product i; Z_i and $Z_{GL} = 3$ represent the number of carbon atoms in the molecule of product i and in the feed GL [31]. Therefore, the calculated selectivities are carbon-based values. The carbon balance (%) was expressed by the ratio of the molar sum (total molar quantities) of detected products (n_i) in the liquid and in the gas phase (CO, CO_2) to the molar amount of converted glycerol (n_{CGL}) (Eq. (3)):

$$C\ (\%) = \frac{\Sigma n_i \cdot Zi}{3} \times \frac{1}{n_{CGL}} \times 100 \quad (3)$$

The products of the dehydration of GL were identified by GC/MS (Varian 3800; OPTIMA WAX, 30 m) coupled with a 1200-TQ mass spectrometer. More details on product identification are given in [28] and in Section 3.3. The absence of thermal dehydration was determined by passing a glycerol–water–helium mixture over 200 mg quartz at standard conditions.

3. Results and discussion

3.1. Textural properties

Table 1 shows the textural data of the binary metal oxides prepared in this study. Catalysts loaded with different metal oxides and phosphates clearly show a decrease in the specific surface area and diameter of the pores with respect to the unloaded support. A reduction of the specific surface area already occurred during modification of the alumina by phosphoric acid. Please note, that the molar relation between metal, alumina and phosphate was kept constant during preparation. The highest loss of specific surface area was observed for the catalysts impregnated with Mn-, Mo- and W-oxide. It amounts to ca. 40% of the initial specific surface area of the support pointing at a deposition of the metal oxide particles within the support pores. These catalysts also exhibited the smallest pores. Moreover, the loss of specific surface area can be partially attributed to the sintering of metal oxide particles during calcination in air at 550 °C on the surface of amorphous Al_2O_3-PO_4.

The existence of the metal oxides, probably as larger particles, is also confirmed by the XRD results shown in Fig. 1. In the case of Ce, Fe, V and Mn modified materials, the reflections of the metal oxides are detected in addition to three very broad reflections of the amorphous aluminium oxide support in the range of 35–65° (2Θ). The Ce-APO sample displays the typical XRD pattern of the cubic structure of CeO_2 (27.6°, 33.2°, 47.4 and 56.3°) [37]. The MO-

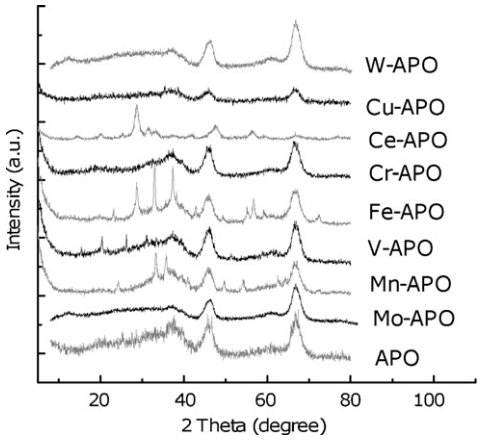

Fig. 1. X-ray diffraction patterns of transition metal-containing phosphated alumina catalysts as well as of APO and AO.

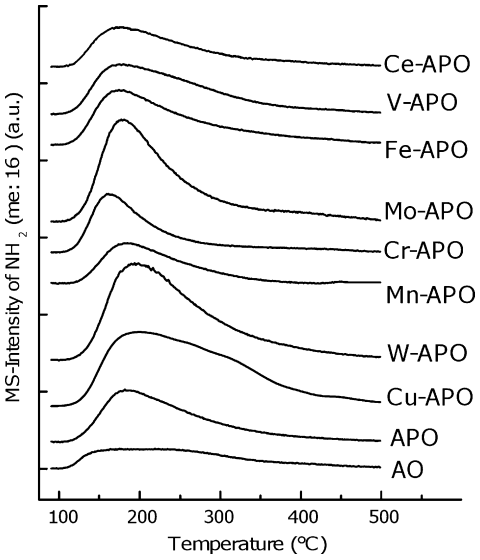

Fig. 2. TPD-profiles of transition metal-containing phosphated alumina catalysts after calcination.

APO system modified with VO_x shows the typical reflexes (15.3°, 20.4°, 26.3°, 31.1° and 34.4°) for vanadium phosphate and V_2O_5 crystallites [38,39]. Mn-APO and Fe-APO composites show also reflexes typical for Fe_2O_3, Fe_3O_4 and MnO_2 or Mn_2O_3, respectively [40,41]. Obviously phases of the amorphous Al_2O_3- or Al_2O_3-PO_4 and crystalline metal oxides segregate during decomposition of the corresponding metal nitrates by the preparation of Fe-APO, Mn-APO and V-APO. This observation is in agreement with the results of Bautista et al. [24], evidencing the formation of Fe-, V- and Mn-oxides in MO–Al_2O_3-PO_4 composites. On the other hand, no reflections associated with crystalline metal oxide phases can be seen in the case of W, Cu and Cr modified samples. This suggests that either the Cr-, Cu- and W-oxides form very fine particles below the detection limits of the XRD or they are incorporated in the framework of the amorphous γ-Al_2O_3 [20,42,43].

3.2. Acidity

It is generally accepted that the catalytic activity in the dehydration of alcohols to olefins is related to the catalyst acidity. Therefore, extensive TPD of ammonia studies were performed for all catalysts to characterize their total acidic properties. According to Tanabe et al. [44] the strength of solid acid sites within TPD profiles can be classified by the temperature of NH_3 desorption as weak (120–300 °C), moderate (300–450 °C) and strong (above 450 °C). The deconvolution of the TPD profiles was difficult, since the profiles do not exhibit several distinct maxima. Instead, TPD profiles with higher intensities in the low temperature region (150–350 °C) were observed (see Fig. 2). Such profiles can be attributed mainly to Lewis acid sites. The surface acidity was calculated as total density of acid sites, further denoted as "total acidity" and expressed as molar amount of NH_3 desorbed per unit mass of catalyst, between 100 and 600 °C (see Table 1). Additionally, the intrinsic acidity is given as molar amount of desorbed NH_3 per unit surface area of the catalyst (see Table 1). The Al_2O_3 support calcined at 520 °C showed a total acidity of 157 μmol g^{-1}. Impregnation of Al_2O_3 with H_3PO_4 resulted in new weak and moderately strong acid sites and the total acidity increased to 295 μmol g^{-1}. Introduction of different transition metal components in Al_2O_3-PO_4 further influenced the total acidity. Incorporation of W, Cu and Mo led to an increased acidity. Other metal oxides, i.e., Cr, Mn, V, Ce, and Fe decreased the total acidity of the catalysts. On the basis of literature results it is difficult to draw reasonable conclusions about the influence of a particular metal component on the materials acidity. The values of the total acidity determined for the investigated catalysts compare reasonably well with that of typical catalysts for glycerol dehydration such as zeolites H-ZSM-5 and alumosilicate supported heteropoly acids with the total acidity of 0.2–0.9 mmol g^{-1} [5,6] and 0.2–0.4 mmol g^{-1} [16], respectively.

The results often depend on the preparation conditions, e.g., calcination temperature, synthesis method, type of precursor, etc. For example, Mishra et al. [23] reported that the acidity of transition metal modified APO catalysts strongly depended on the calcination temperature and not exclusively on the type of metal. Non-modified APO was found to be less acidic than metal modified catalysts [23]. However, the experiments were carried out by adsorption of pyridine from a cyclohexane solution at room temperature and analysis of consumed pyridine molecules. On the other hand, Bautista et al. [24] reported that Fe-modified APO exhibited lower acidity than pure APO. Our results confirm the general agreement that total acidity, which is predominant for the investigated catalysts, is directly related to Pauling electronegativity of the transition metal [44]. W, Mo and Cu exhibit the highest electronegativity in the row of studied materials; thus, they also show the highest acidity. The lower electronegativities of Fe, Cr, Mn, V and Ce correlate with similar or lower acidities in comparison to the non-modified APO.

3.3. Catalytic conversion of glycerol

The glycerol conversion, the selectivities to acrolein and acetol as well as the main identified by-products and the carbon balance are presented in Table 2 for a TOS of 1 h and for steady state conditions at TOS of 30 h at 280 °C. The results of catalytic experiments show that all investigated catalysts except the alumina precursor (Al_2O_3-PO_4) exhibit essentially full conversion of glycerol after 1 h TOS.

The low conversion of GL over AO is attributed to its low acid-site density. High selectivity towards acrolein was observed for Cu-, W- and Mo-modified catalysts as well as for the transition metal-free APO. In contrast, Ce- and Mn-modified materials showed higher selectivity to other desired products, e.g., acetol. APO modified with Cr and Fe exhibited moderate selectivities either to acrolein or acetol. On these catalysts, the formation of numerous side products including phenol, acetaldehyde, allyl alcohol and CO_x (mainly CO) was observed. In addition to that, traces of various other by-products were detected.

By-products with selectivities of more than 0.8% were identified by GC–MS analysis. Detailed information about the formation of by-

Table 2
Conversion of glycerol and product distribution over different MeO-APO catalysts[a]. Reaction conditions *T*: 280 °C; GHSV: 75 h^{-1}; glycerol: 1 g h^{-1} (5 wt% solution); Cat.: 200 mg; He: 100 ml min^{-1}.

Catalyst	TOS (h)	*X* (%)	Selectivity (%)								C-Balance (%)[f]
			Acrolein	Acetol	Phenol	AcH[b]	AA[c]	CO_x	AOH[d]	Others	
AO [e]	1/10	11/5	25/20	32/25	3/1	2/2	0/0	1/0	0/0	37/52	80/92
APO[e]	1/10	100/69	62/35	4/30	8/7	4/3	0/0	2/1	1/0	20/23	91/94
Cu-APO	1/30	100/96	73/23	2/50	10/6	4/3	3/2	3/3	1/1	3/12	93/95
Ce-APO	1/30	70/38	12/10	58/45	4/1	3/6	2/2	2/1	2/2	17/33	90/92
Cr-APO	1/30	100/99	21/10	5/42	28/23	8/11	6/4	10/3	2/1	20/6	94/95
Fe-APO	1/10	92/50	23/15	15/21	6/3	4/12	3/2	9/5	10/15	29/27	90/93
Mo-APO	1/30	98/90	54/45	10/23	9/4	5/3	3/4	5/3	3/5	8/12	93/97
Mn-APO	1/30	100/88	17/10	42/26	5/3	7/6	2/2	12/18	1/0	14/35	91/93
W-APO	1/30	100/99	61/54	14/28	11/3	2/3	2/3	3/2	1/2	5/5	95/96
V-APO	1/30	100/100	20/15	14/10	9/5	8/7	6/5	11/15	23/21	9/21	90/94

[a] Conversion and selectivity were analysed for products obtained during the initial 1 h of reaction. Data after back slash were analysed for products obtained from 28 to 30 h of reaction.
[b] Acetaldehyde.
[c] Acrylic acid.
[d] Allyl alcohol.
[e] After reaction time of 10 h.
[f] Carbon-balance.

products is described in detail in a previous work [28]. By-products grouped under the label of "others" (Table 2) include propionic acid, acetic acid, acrylic acid, acetone, propionaldehyde, glycidol and various cyclic products such as 3-methylfuran, 2,3-dimethylfuran, C_6-lactone and cyclic acetal derivatives [28]. The selectivities of each one were lower than 2–3%. Thus, these by-products are not further discussed in the present work.

The calculated C-balance was usually above 98% after TOS of 1 h. After steady-state conditions have been reached, the C-balance between 93 and 96% for most of the MO_x–Al_2O_3-PO_4 catalysts suggested no relevant formation of heavy compounds on the surface of catalysts or other unknown products. The C-balance for pure alumina, Al_2O_3-PO_4 and CeO_x–Al_2O_3-PO_4 was below 90%, which indicates a significant formation of heavy compounds on the surface of the catalysts ("coke") possibly also responsible for a rapid deactivation after a TOS of 10 h.

A high amount of phenol was observed in the reactions product for the W- and Cr-modified materials. This phenomenon is obviously associated with the destructive C–C-cleavage of 3-hydroxyl-propionaldehyde to acetaldehyde followed by cyclization to phenol [45]. The formation of phenol during the conversion of GL was previously reported by Dubois et al. [19] and Prieto [46]. They found that the phenol formation is strongly dependent on the reaction conditions, e.g., the concentration of GL in the aqueous feed solution, the temperature and the contact time.

The formation of acrylic acid, acetic acid and propionic acid was also described in the literature and some patents in the context of glycerol conversion in absence of molecular oxygen over supported heteropoly acids, transition metal ion containing catalysts (Mo, W, Ce) and zeolite ZSM-5 [9,19,20,47–49]. However, exact data about selectivities towards these C_2–C_3 carboxylic acids are not listed. The formation of acids can be attributed to the oxidation reaction of C_2–C_3–aldehydes with framework oxygen of the catalysts. Oxidation with active lattice oxygen is also believed to be responsible for the generation of CO_x via oxidative cleavage of intermediate products [2,3,25,26,29].

A low selectivity to acrolein and acetol was observed on APO loaded with VO_x (20 and 14%, respectively). Instead, a selectivity of over 20% to allyl alcohol as well as the formation of acetaldehyde, acrylic acid, CO_x and other unidentified products was found. Such product distribution suggests that VO_x is particularly active towards oxidation. Formation of allyl alcohol with a selectivity of 5–7% was also observed in the case of FeO_x containing APO.

The conversions at 1 and 10 h time-on-stream (100 and 63%, respectively) show a gradual deactivation of unmodified APO. Additionally, a change in the selectivity from acrolein to acetol was observed. The same shift in selectivity to the desired dehydration products was found for all catalysts modified with transition metals except for Mn-APO which exhibited a higher selectivity towards acetol already in the beginning of the reaction. Apart from Ce-APO, all other metal oxide-containing catalysts retained full conversions. A lower activity and deactivation of Ce-modified material can be explained by the lowest acid site density (see Table 1), weak redox properties at lower temperatures and slight basicity [26,50]. This is also confirmed by a comparison of coke formation after 30 h over all studied catalysts (see Table 1). Ce-APO clearly exhibited the highest coke formation comparable to unmodified APO, while the coke deposition over the other transitions metal-oxide modified catalysts was generally lower. The amount of deposited coke also correlates well with the loss of the specific surface areas of the studied catalysts. The alumina precursor (AO), the phosphated alumina (APO) and Ce-APO show the strongest loss of the specific surface area during reaction, i.e., 53, 46 and 41%, respectively (see Table 1). In contrast, the other metal containing catalysts exhibit a much lower decrease in the specific surface area in the range of 12–22%.

These results show the importance of acid and redox properties of the catalysts for the conversion of GL and the product distribution. It can be concluded that a high acid site density is a prerequisite for an initially high conversion, while the presence of a transition metal component mainly influences the catalytic stability and the product distribution.

The results presented above were obtained at 280 °C in which the catalysts exhibited nearly complete conversion for most of the studied catalysts. To get more insight into the influence of catalyst acidity on the conversion of GL, the catalytic experiments were additionally carried out at 265 °C. Fig. 5a and b shows the catalytic activity and selectivity for acrolein after 1 h. The measurements were performed in the initial period of the reaction in order to reduce the influence of the deactivation. The results clearly indicate the dependence of the initial conversion on the acidity of the catalysts (see Fig. 3a). Catalytic activity, increased with the increase of the intrinsic catalyst acidity; i.e., conversion of GL increased in the order: Ce < Mn < Cr < V ≈ Fe < Cu < Mo < W. Thus, weakly acidic Ce- and Mn-APO catalysts exhibited the lowest conversion and strongly acidic W-, Mo- and Cu-APO catalysts exhibited highest conversion. Moreover, the high intrinsic acidity also correlates well with the

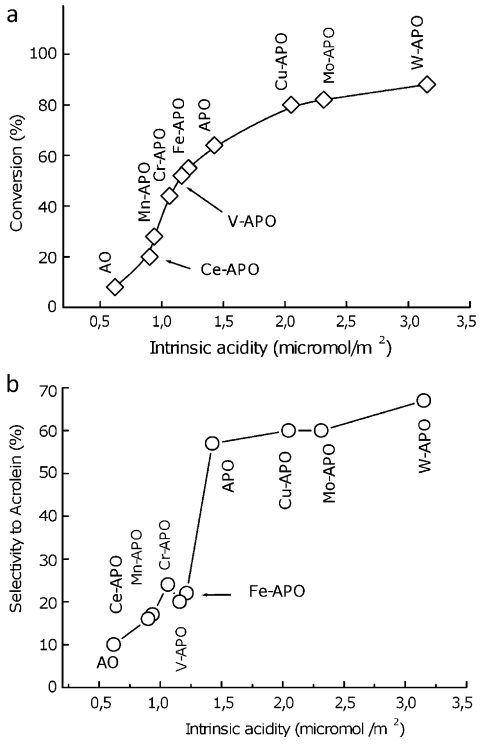

Fig. 3. Dependence of the glycerol conversion (a) and selectivity for acrolein (b) on the intrinsic acidity for different catalysts at 265 °C. TOS = 60 min.

selectivity to acrolein (see Fig. 3b). These results confirm a more general hypothesis about the substantial role of the acid properties of the catalyst in the selective conversion of GL to acrolein [3,7]. However, it needs to be mentioned that all catalysts exhibit acid sites of weak or moderate strength only, presumably of the Lewis type. Chai et al. [11,32] claimed that the selective conversion of GL to acrolein over APO and other acidic catalysts proceeds mostly due to very strong Brønsted acid sites of these catalysts. This suggestion is in contradiction to our previous results [28], which indicate that APO possesses predominantly weak or moderate acidic sites. Moreover, strong Brønsted acid sites can be detrimental in the long-term as the formation of many side-products due to decomposition of instable intermediates and oligomerization of glycerol and acrolein occurs [12,28,50]. Similarly, Ulgen and Hoelderich [20] found no direct correlation between the selectivity for acrolein and the total amount of acid sites. They attributed this result rather to the influence of weak acid sites and the absence of basic sites.

The higher selectivity to acetol formation in the dehydration of glycerol over binary oxide catalysts containing Sn, Ti, Al and Zr was explained by Tao et al. [51] as an effect of basic sites coexisting on the surface of the catalysts and their involvement in the dehydration reaction. All these inconsistencies suggest that acidity and basicity of the catalysts constitute only as one factor affecting the catalytic activity and selectivity and other catalyst properties, e.g., dispersion and redox activity of the metallic component play an equally important role [23,24,52].

Fig. 4 shows the conversion of glycerol for longer TOS over selected catalysts, i.e., Cu-, W-, V-APO and unmodified APO. While GL conversion over APO gradually decreases due to deactivation, the catalysts modified with Cu and W show prolonged stability with only a slight decrease in conversion after ca. 5–10 h followed by a gradual increase in the later stages of catalytic run. This unusual behaviour is especially pronounced in the case of the catalyst modified with Cu. Closer inspection of selectivity profiles reveals an inversion of the selectivity from acrolein to acetol at the time of

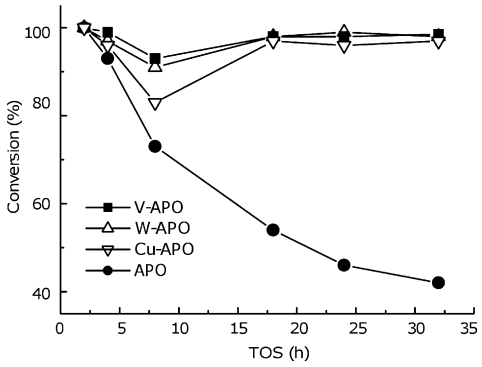

Fig. 4. TOS-conversion profiles over APO, W-APO, V-APO and Cu-APO catalysts at 280 °C.

the decrease of conversion (see Fig. 5a and b). This result suggests the transformation of the active surface sites of the metal oxide on the support into another type of site which favors a different reaction pathway. The fact that unmodified APO exhibits only a gradual deactivation clearly indicates the role of the metal component in this process.

Sato et al. [29] observed that, in the presence of a copper oxide catalyst, the main product of glycerol conversion is acetol. It is known that in the presence of copper oxide, the dehydration proceeds via the formation of Cu-alkoxide species via hydrogen abstraction from the secondary hydroxyl groups [53,54]. The alkoxide produced from GL can release an OH radical from the primary OH groups to yield acetol. Cu-alkoxide species can also be formed via interaction with primary hydroxyl groups. In this case, acetol can also be obtained. However, the formation of acrolein is possible, too. Sato et al. [26,29] proposed that the acidity of the support is crucial for the product distribution and that a high acid sites density promote the formation of acetol. This explanation supports our findings regarding increasing intrinsic acidity of the bifunc-

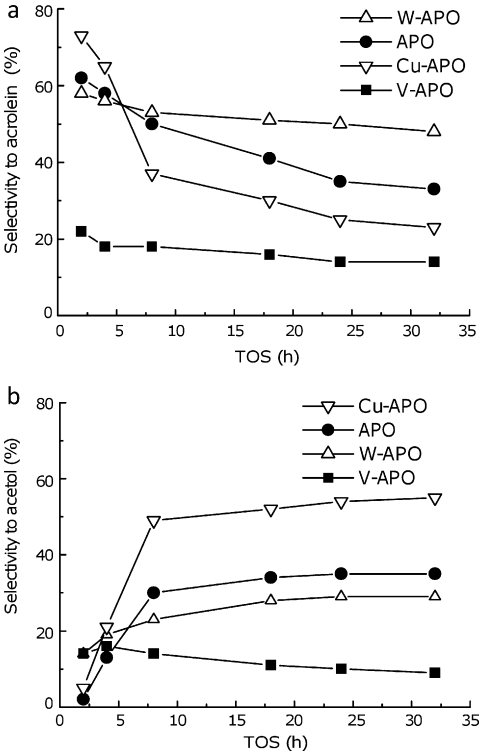

Fig. 5. Selectivity as a function of TOS for acrolein (a) and acetol (b) APO, W-APO, V-APO and Cu-APO catalysts at 280 °C.

tional catalysts in the course of the reaction due to the presence of redox components accompanied by increasing selectivity to acetol. In the presence of strong acidic centers, the abstraction of a terminal HO-radical from the metal alkoxide species, although less favored thermodynamically, is statistically more probable.

Generally, V-APO generally exhibits very low selectivities to acrolein and acetol and does not follow the trend of Cu- and W-APO catalysts. In the case of V-APO, allyl alcohol is the main product and its formation increases over time on stream. We also observed the same phenomenon for Fe-APO (see Table 2).

The exact role of vanadia or iron oxide in the process of allyl alcohol formation is not clear. Kijenski et al. [55] found that allyl alcohol forms during GL dehydration over acidic redox catalysts, e.g., SO_4–Fe_2O_3–SiO_2. In the course of destructive oxidation of acrolein or acetaldehyde the formation of formic acid occurs, which then undergoes esterification with glycerol followed by dehydration and hydrolysis of formiate to form allyl alcohol. Participation of formic acid was also confirmed by Arceo et al. [56]. Recently, Schueth and co-workers [34] reported the process of allyl alcohol production from GL over phosphorus containing Fe_2O_3 nanoparticles (iron oxide–$Al(H_2PO_4)_3$ mixed catalyst). Although the exact mechanism is not finally explored, the authors suggest that the formation of allyl alcohol proceeds via dehydration and consecutive hydrogen transfer.

3.4. Active sites in the catalytic dehydration of glycerol

Several types of active sites coexist on the surface of investigated catalysts. This includes acidic function which is associated predominantly with PO_4 surface groups, and redox function which can be assigned to metal oxide component. Both of them however finely interfere with each other. Thus, it is difficult to assess their role in the glycerol dehydration separately. In order to clarify their role in the glycerol conversion and the product distribution, detailed investigations using TPD, TPR and XPS were carried out for Cu-, W-, and V-containing APO catalysts. These three metals were selected, because the corresponding catalysts show different behaviour with respect to formation of the desired products acrolein, acetol and allyl alcohol (see Table 2).

3.4.1. Acidic sites

First of all, we investigated the change in the acidic properties of the fresh catalysts and after dehydration of glycerol at 280 °C after 30 h TOS. Fig. 6 shows the comparison of total acidity for Cu-, W-, and V-containing catalysts as well as the unmodified APO. In the case of APO, a strong decrease of ca. 60% in total acidity was observed after the dehydration reaction. A slight decrease in total acidity was also observed for the Cu-modified catalyst. In contrast, the total acidity of W- and V-modified APO catalysts increased for ca. 10–20%.

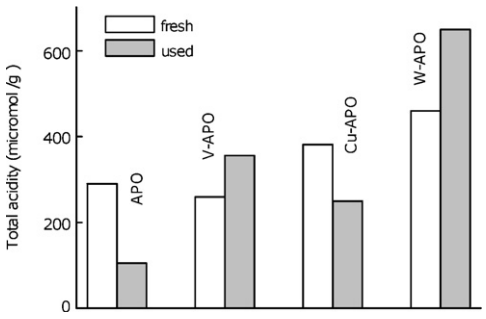

Fig. 6. Comparison of the total acidity of catalysts before (fresh) and after reaction (used) with glycerol at 280 °C for 30 h TOS.

The comparisons of the results of ammonia TPD before and after the reaction are presented in Fig. 7a–d. It is clearly visible that the formation of new strong acidic sites occurs in the course of the reaction which is accompanied by the decrease of the low temperature maximum at 180–250 °C present in the fresh catalysts. In the case of W- and V-containing APO, the newly formed strong acidic centers, presumably of the Brønsted type, appear in the temperature region of 300–450 °C with a maximum at ca. 380 °C. The Cu-containing APO shows a similar occurrence of strong acid sites after the reaction, but in a lower amount and with an additional maximum at 460 °C. Upon repeated calcination of the used catalyst at 550 °C in air, the strong acid sites disappear and the low-temperature maximum in the TPD-profile is recovered. This suggests that the strong acid sites formed in the course of the reaction are of organic nature. The formation of "new" acidic sites may be the reason for the change in the selectivity from acrolein to acetol (cf. above). It also confirms the suggestion made by Chai et al. [11], Ulgen and Hoelderich [20] and Alhanash et al. [14] associating the high selectivity for acrolein with the weak acid sites of the catalyst.

Dehydration of GL proceeds with the formation of acrolein, acetol and many side products, e.g., C_2–C_3 carboxylic acids. Acrylic acid possibly formed by oxidation of acrolein with framework oxy-

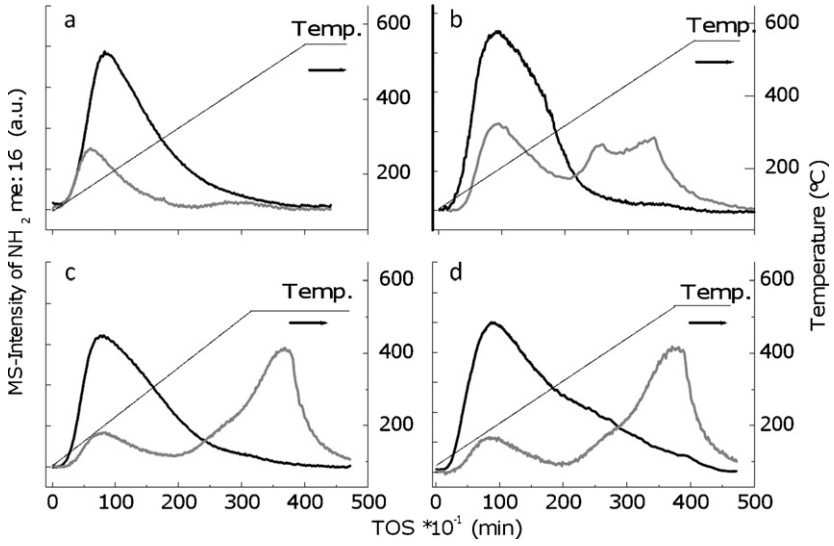

Fig. 7. NH_3-TPD profiles of MO_x-APO catalysts before (black) and after dehydration of glycerol (gray) at 280 °C for 30 h TOS. (a) APO; (b) Cu-APO; (c) V-APO; (d) W-APO.

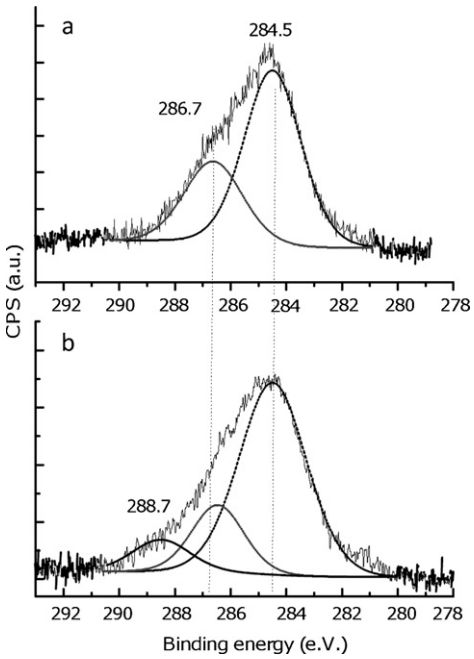

Fig. 8. XPS spectra of APO (a) and V-APO catalyst (b) in the C 1s region after treatment with a glycerol–water flow at 280 °C for 30 h TOS.

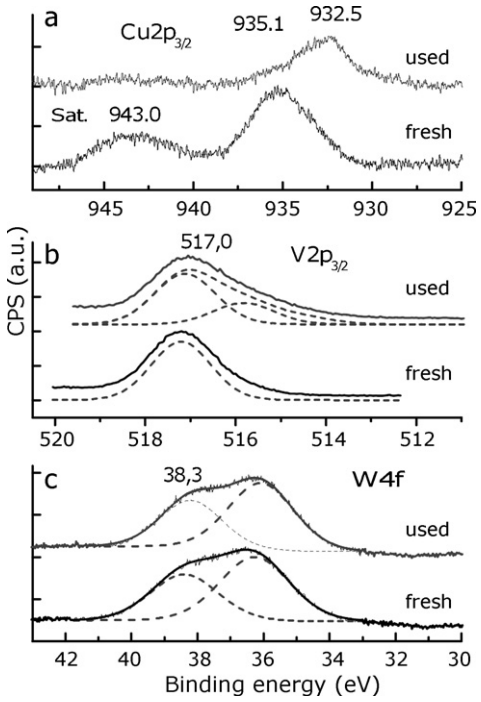

Fig. 9. XPS spectra of Cu-APO (a), V-APO (b) and W-APO (c) before (fresh) and after treatment (used) with glycerol–water flow at 280 °C for 30 h TOS.

gen can polymerize to polyacrylic compounds covering the catalyst surface [57] and inducing additional Brønsted acidity. These acidic compounds contribute to the total acidity of the used catalysts, partially blocking the originally present weak acid sites on the catalyst surface as confirmed by the decrease of the maximum in the lower temperature region of the TPD spectra. The formation of strong Brønsted-acid sites was not observed in the case of the unmodified APO which does not possess active framework oxygen able to oxidize reaction products (see Fig. 7a).

The formation of different oxygenated carbon compounds on the catalyst surface after the reaction was also confirmed by XPS analysis (Fig. 8a and b). In the case of the unmodified APO, two different C 1s components at 284.5 eV and 286.3 eV were observed in the C 1s region of XPS. The first signal can be assigned to C–C bonds of the coke deposit, while the second one is attributed to a C–O–C bond of oxygenated coke deposits originating from oligo- and polyglycerol and polyacrolein. Fig. 8b shows the same XPS region for V–containing APO. In this case, apart from the peaks at 284.5 eV and 286.3 eV, an additional peak at higher binding energy of 288.3 eV was found. Such a high shift of the C 1s signal is often attributed in the literature to carboxylic species [58], which confirms the suggestion of the formation of polyacrylic acid on the surface of the transition metal containing APO. The presence of a C 1s signal at high binding energies was also observed for W-and Cu-containing catalysts.

3.4.2. Redox sites

XPS and TPR experiments were carried out to clarify the role of the metal oxide component in the catalytic activity and selectivity. The XPS spectra of the Cu $2p_{3/2}$, W 4f and V $2p_{3/2}$ regions of the fresh and used catalysts presented in Fig. 9a–c reveal different oxidation states of the metallic components on the surface. The most significant difference is visible for the Cu–containing catalyst. (see Fig. 9a). The fresh catalyst shows the presence of copper mainly in the oxidation state +2 with a binding energy (BE) of 934.6 eV and a distinct shake-up satellite at 943 eV typical for CuO. Deconvolution of the main signal revealed an additional small component at 932.6 eV, which can be assigned to copper in the oxidation state +1. After reaction the signal of Cu $2p_{3/2}$ shifts to a lower BE of 932.7 eV. Additionally, the shake-up satellite disappears. The observed low signal-to-noise ratio is due to the fact that only 1 at.% of Cu is present on the external catalyst surface. The main signal at 932.7 eV cannot be unambiguously associated with Cu in the oxidation state +1 or ±0 as both, Cu(+) and Cu(0) appear at similar binding energies and lack shake-up satellites. Nevertheless, the results show the reduction of copper during dehydration of GL.

The XPS spectra of V-APO before and after catalytic dehydration of GL showed a slight difference in the shape of the V $2p_{3/2}$ signal (see Fig. 9b). In particular, a pronounced tailing at lower binding energies was observed, although the maximum of the signal at 517.1 eV remained unchanged. Deconvolution of the signals revealed an additional component at lower BE of 515.8 eV which can be assigned to a reduced vanadium species in the oxidation state +4 or +3. This low BE signal was more intense in the case of the used catalyst suggesting partial reduction of V species during dehydration of GL. In contrast, a reduction of W oxides in W-APO during the catalytic reaction could not be confirmed by XPS. The characteristic doublet of W 4f with a maximum for component W $4f_{7/2}$ at 36.1 eV remains unchanged even after the reaction (see Fig. 9c). This finding stays in agreement with the common knowledge that tungsten oxide is more difficult to reduce in comparison to copper oxide [29,59]. On the other hand, Volta [60] and Sato et al. [26] proposed a possible reoxidation of metal oxide species in the presence of water, which can be an additional explanation for the lack of pronounced reduction after the reaction.

Further information about the redox state of the metallic component on the M-APO catalysts was obtained from H_2-TPR experiments. The results confirmed XPS findings regarding partial reduction of copper oxide and vanadium oxide species on the surface of the catalysts in the course of the reaction. W-containing catalyst could not undergo reduction under experimental conditions, as it requires temperature above 800 °C—not obtainable with our setup. Nevertheless, TPR profiles revealed small changes in WO_x species after the reaction, i.e., partial transformation of octahedrally coordinated species into tetrahedral as well as partial aggregation

of surface species into bulky WO_3 clusters. Details of TPR experiments, including figures, are presented in the supplementary part.

XPS, TPR and NH_3-TPD are not sufficient for the verification of the type of active sites. Future work will focus on FTIR investigations of fresh and used catalysts with adsorbed pyridine allowing distinguishing between Brønsted and Lewis sites.

4. Conclusions

The catalytic performance of hydrothermally stable bifunctional catalysts containing different transition metal oxides on acidic phosphated alumina was studied for the gas-phase dehydration of glycerol in an excess of water at constant reaction conditions. The presence of the metal oxide influenced the total and intrinsic acidity of the phosphated alumina catalysts and their performance.

It was found that several factors contribute to the performance of these catalysts. There is a direct correlation between the intrinsic acidity and the catalyst performance: the higher the acidity, the higher the glycerol conversion as well as the selectivity towards acrolein. Additionally, the presence of transition metal oxides, i.e., redox centers, leads to an efficient removal of organic deposits from the surface, thus lowering deactivation. Redox centers also influence the product distribution, in particular, MoO_x- and WO_x–Al_2O_3-PO_4 systems show the highest long term catalytic activity and because of its high acidity high selectivity to acrolein. In contrast, Cu-, Cr- and Ce-oxide containing catalysts characterized by lower acidity favor the formation of acetol. The highly active redox sites of Cr-, Fe-, Mn- and V-oxides favor the oxidation of primary reaction products, leading to formation of carboxylic acids. Further oxidation leads to products of C–C-bond cleavage such as acetaldehyde and CO_x.

It was found that the conversion of glycerol and the selectivity towards desired products (acrolein and acetol) as well as the total acidity of the catalysts changed with time on stream. In contrast to the pure acidic catalyst (Al_2O_3-PO_4), where the acidity decreased with time on stream, evolution of new type of acidic sites was observed on transition metal oxide containing catalysts, assumedly due to formation of carboxylic species on the catalyst surface. However, the total acidity of spent transition metal oxide containing catalysts decreased in most cases. The observed change in product distribution with time on stream is in agreement with the decreasing acidity of the spent catalysts. A change of the oxidation state of easily reducible metal oxides such as Cu-oxide, and/or a phase transformations of the metal oxides also influenced the product distribution.

The presented results demonstrate that promotion of phosphated alumina with transition metal oxides effectively influences the reaction pathways of the catalytic gas-phase conversion of glycerol. Both, acidity and redox properties of the catalyst are important factors for conversion and product distribution. A sensitive tuning of these two properties may be the key to further improvement of activity, selectivity and stability of catalysts for the catalytic conversion of glycerol to desired products.

Acknowledgment

Financial support was provided by Deutsche Forschungsgemeinschaft (DFG).

Appendix A. Supplementary data

Supplementary data associated with this article can be found, in the online version, at doi:10.1016/j.molcata.2011.04.020.

References

[1] A. Behr, J. Eilting, K. Irawaldi, J. Leschinski, F. Lindner, Green Chem. 10 (2008) 13–20.
[2] Y. Zheng, X. Chen, Y. Shen, Chem. Rev. 108 (2008) 5253–5277.
[3] B. Katryniok, S. Paul, V. Belliere-Baca, P. Rey, F. Dumeignil, Green Chem. 12 (2010) 2079–2098.
[4] M.M. Bettahar, G. Costentin, L. Savary, J.C. Lavalley, Appl. Catal. A: Gen. 145 (1996) 1–48.
[5] Y.T. Kim, K.-D. Jung, E.D. Park, Appl. Catal. A: Gen. 393 (2011) 275–287.
[6] J.T. Kim, K.-D. Jung, E.D. Park, Micropor. Mesopor. Mater. 131 (2010) 28–36.
[7] C.J. Jia, Y. Liu, W. Schmidt, A.H. Lu, F. Schueth, J. Catal. 269 (2010) 71–79.
[8] A. Corma, W.H. Huber, L. Sauvanaud, P. O'Connor, J. Catal. 257 (2008) 163–171.
[9] A. Caldarelli, F. Covani, F. Folco, S. Lucani, C. Cortelli, R. Lenza, Catal. Today 157 (2010) 204–210.
[10] H. Redlingshöfer, C. Weckbecker, K. Huthmacher, A. Dörflein, Pat. DE 102007 004 351 A1 2008.07-31. Neue Katalysatoren und Verfharen zu Dehydratisierung von Glycerin.(Evonik Degussa).
[11] S.-H. Chai, H.-P. Wang, Y. Liang, B.-Q. Xu, Green Chem. 9 (2007) 1130–1136.
[12] W. Yan, G.J. Suppes, Ind. Eng. Chem. Res. 48 (2009) 3279–3283.
[13] L. Ott, M. Bicker, H. Vogel, Green Chem. 8 (2006) 214–220.
[14] A. Alhanash, E.F. Kozhevnikova, I.V. Kozhevnikov, Appl. Catal. A: Gen. 378 (2010) 11–18.
[15] E. Tsukuda, S. Sato, R. Takahashi, T. Sodesawa, Catal. Commun. 8 (2007) 1349–1353.
[16] H. Atia, U. Armbruster, A. Martin, J. Catal. 258 (2008) 71–82.
[17] L. Ning, Y. Ding, W. Chen, L. Gong, R. Lin, H. Lü, Q. Xin, Chin. J. Catal. 29 (2008) 212–214.
[18] U. Armbruster, H. Atia, A. Martin, Chem. Ing. Technol. 82 (2010) 1203–1210.
[19] J. L. Dubois, C. Duquenne, W. Hoelderich, J. Kervenal, Pat. WO: 2006/087084 A2 Process for dehydration of glycerol to acrolein (Akrema).
[20] A. Ulgen, W. Hoelderich, Catal. Lett. 131 (2009) 122–128.
[21] J.M. Campelo, A. Garcia, J.F. Herencia, D. Luna, J.M. Marinas, A.A. Romero, J. Catal. 151 (1995) 214–307.
[22] S.C. Laha, G. Kamalakar, R. Gläser, Micropor. Mesopor. Mater. 90 (2006) 45–52.
[23] T. Mishra, K.M. Parida, S.B.R. Raom, Appl. Catal. A: Gen. 166 (1998) 115–122.
[24] F.M. Bautista, J.M. Campelo, A. Garcia, D. Luna, J.M. Marinas, R.A. Quiros, A.A. Romero, Appl. Catal. A: Gen. 243 (2003) 93–107.
[25] S.Y. Liu, C.J. Zhou, Q. Li, G.C. Lium, C.L. Huang, Z.S. Chao, ChemSusChem 1 (2008) 578–581.
[26] S. Sato, R. Takahashi, T. Sodesawa, N. Honda, J. Mol. Catal. A: Chem. 221 (2004) 177–183.
[27] Q. Liu, Z. Zhang, Y. Du, J. Li, X. Yang, Catal. Lett. 127 (2009) 419–428.
[28] W. Suprun, M. Lutecki, T. Haber, H. Papp, J. Mol. Catal. A: Chem. 309 (2009) 71–78.
[29] S. Sato, M. Akiyama, R. Takahashi, T. Hara, K. Inui, M. Yokota, Appl. Catal. A: Gen. 347 (2008) 186–191.
[30] J. Delaplanque, J.-L. Dubois, J.-F. Devaux, W. Ueda, Catal. Today 157 (2010) 351–358.
[31] F. Wang, J.L. Dubois, W. Ueda, J. Catal. 268 (2009) 260–267.
[32] S.-H. Chai, H.-P. Wang, Y. Liang, B.-Q. Xu, J. Catal. 250 (2007) 342–349.
[33] S. Erlfe, U. Armbruster, U. Bentrup, A. Martin, A. Brückner, Appl. Catal. A: Gen. 391 (2011) 102–109.
[34] Y. Liu, H. Tüysüz, C.-J. Jia, M. Schwickardi, R. Rinaldi, A.H. Lu, W. Schmidt, F. Schueth, Chem. Commun. 46 (2010) 1238–1240.
[35] W. Suprun, R. Gläser, H. Papp, Gasphasen Dehydratisierung von Glycerol an bifunktionellen Katalysatoren, Deutsche Wissenschaftliche Gesellschaft für Erdöl, Erdgas und Kohle; DGMK–Tagungsbericht. (2010) 2010–2012, pp. 307–314.
[36] W. Suprun, H. Papp, Gas-phase conversion of glycerol over mixed metal oxide catalysts, Catal. Ind. 3 (1) (2011) 70–75.
[37] G.D. Angel, J.M. Padilla, I. Cuauhtémoc, J. Navarette, J. Mol. Catal. A: Chem. 281 (2008) 173–178.
[38] E.P. Reddy, R.S. Varma, J. Catal. 221 (2004) 93–101.
[39] X.H. Taufiq-Yap, Y.C.K. Goh, G.J. Hutchings, N.B. Dummer, Catal. Lett. 130 (2009) 327–334.
[40] W.M. Shaheen, K.S. Hong, Thermochim. Acta 381 (2002) 153–164.
[41] F. He, H. Wang, Y. Dai, J. Nat. Gas Chem. 16 (2007) 155–161.
[42] H. Nair, M.J. Liszka, J.E. Gatt, C.D. Baertsch, J. Phys. Chem. C 112 (2008) 1612–1620.
[43] V.M. Benitez, C.A. Querini, N.S. Figoli, Appl. Catal. A: Gen. 252 (2003) 427–436.
[44] K. Tanabe, M. Misono, Y. Ono, H. Hattori, Stud. Surf. Sci. Catal. 51 (1989) 5–25.
[45] I.J. Miller, E.R. Saunders, Fuel 66 (1987) 130–135.
[46] S.S. Prieto. Optimization of the dehydration of glycerol to acrolein and a scale up in a pilot plant; Ph.D. Thesis, RWTH, Aachen2008 Metadata Internet Doc. http://www.meind.de/search.py?recid=387582.
[47] A.K. Kinage, P.P. Upare, P. Kasinathan, Y.K. Hwang, J.-S. Chang, Catal. Commun. 11 (2010) 620–623.
[48] W. Hölderich, A. Ülgen, Pat. DE 10 2008 031 727, A1; 2010.01.07 and Pat. DE 10 2008 031 828 A1; 2010.01.07.
[49] L. Cheng, X.-P. Ye, Catal. Lett. 130 (2009) 100–109.
[50] H. Gotoh, Y. Yamada, S. Sato, Appl. Catal. A: Gen. 377 (2010) 92–98.
[51] L.-Z. Tao, S.-H. Chai, Y. Zuo, W.-T. Zhneg, Y. Liang, B.-Q. Xu, Catal. Today 158 (3–4) (2010) 310–316.
[52] E. Iglesia, D.G. Barton, J.A. Biscardi, M.J.L. Gines, S.L. Soled, Catal. Today 38 (1997) 339–360.

[53] A.J. Gellman, M.T. Buelow, S.C. Street, T.H. Morton, J. Phys. Chem. A 104 (2000) 2476–2485.
[54] R.M. Rioux, M.A. Vannice, J. Catal. 216 (2003) 362–376.
[55] J. Kijeński, A. Migdał, O. Oswaru, E. Śmigiera, Pat. Method for processing, the glycerol phase from transesterification of fatty acid triglycerols (Insitut Chemii Przemyslowej), Warszawa (Pl) EP 1860090 A1, 2006.
[56] E. Arceo, P.P. Marsden, R.G. Bergman, J.A. Ellman, Chem. Commun. 23 (2009) 3357–3359.
[57] S. Dubinsky, G.S. Grader, G.E. Shter, M.S. Silverstein, Polym. Degrad. Stabil. 86 (2004) 171–178.
[58] N. Wu, L. Fu, M. Su, M. Aslam, K.C. Wong, V.P. Dravid, Nano Letters 4 (2004) 383–386.
[59] V. Logie, G. Maire, D. Michel, J.L. Vignesy, J. Catal. 188 (1999) 90–101.
[60] J.C. Volta, Top. Catal. 15 (2–4) (2001) 121–129.